

5-2024

Modeling Group 3 Medulloblastoma: Describing the Interconnected Pathway of the Most Common Pediatric Brain Cancer

Amber Cantú
William & Mary

Follow this and additional works at: <https://scholarworks.wm.edu/honorsthesis>



Part of the [Computational Chemistry Commons](#)

Recommended Citation

Cantú, Amber, "Modeling Group 3 Medulloblastoma: Describing the Interconnected Pathway of the Most Common Pediatric Brain Cancer" (2024). *Undergraduate Honors Theses*. William & Mary. Paper 2149. <https://scholarworks.wm.edu/honorsthesis/2149>

This Honors Thesis -- Open Access is brought to you for free and open access by the Theses, Dissertations, & Master Projects at W&M ScholarWorks. It has been accepted for inclusion in Undergraduate Honors Theses by an authorized administrator of W&M ScholarWorks. For more information, please contact scholarworks@wm.edu.

Modeling Group 3 Medulloblastoma: Describing the Interconnected

Pathway of the Most Common Pediatric Brain Cancer

A thesis presented in Candidacy for Departmental Honors in

Neuroscience

from

The College of William and Mary in Virginia

By

Amber Nicole Cantú

May 6, 2024

Accepted for

Honors

Randolph Coleman

Dr. Randolph A. Coleman

Christy Porter

Dr. Christy Porter

Jorge Terukina

Dr. Jorge Terukina

Table of Contents

Author Note	4
Abstract.....	5
Introduction.....	6
Molecular Actors and Their Roles.....	6
BCL-xL	7
NRL & CRX	8
NRL	8
CRX.....	9
NRL & CRX	9
IL-6 and JAK/STAT Signaling Pathway.....	10
OTX2.....	10
Hypothesized Pathway of Molecular Events	11
Methods.....	12
Cell Designer & SBML Squeezer.....	13
Data	13
COPASI.....	14
Results	14
Limitations.....	17
Discussion.....	18

Maternal Diet and Disease	18
Treatments	21
Medicine.....	21
Diet	22
Conclusion	23
References	25
Appendix A	29
Appendix B	33

Author Note

Funded by the Charles E. Flynn '34 Memorial Chemistry Scholarship

Supported by the Charles Center

Abstract

Group 3 medulloblastoma is one of the most common pediatric brain cancers. Affecting infants and children, this cancer has the worst prognosis of the medulloblastoma group. Current treatments use surgical resection, radiation, and chemotherapy to afflict the cancer, however no cure has been found. This project aims to model one of the many pathways being investigated in Group 3 medulloblastoma which may be used to synthesize future treatments. Specifically, showing the interconnections between various precursors of BCL-xL, an antiapoptotic protein, and how these factors influence the progression of the disease. Scientific databases were used to find previous research articles which were analyzed for qualitative and quantitative information. *In silico* modeling and simulation of biochemical processes were performed by CellDesigner and COPASI, respectively. These methods were used to represent and quantify the overall pathway. It was found that BCL-xL inhibits the formation of the BAX pore and is modulated by NRL and its precursors OTX2 and CRX as well as the IL-6 pathway. This project shows that increased concentrations of intracellular OTX2, NRL, CRX, and IL-6 lead to increased BCL-xL concentrations and promote BCL-xL binding with the BAX pore subunits, inhibiting apoptosis. This pathway supports previous hypotheses for Group 3 medulloblastoma cancer cell progression by modeling the biochemical pathway that prevents cell death. Interestingly, an external factor that has been found to possibly influence this pathway is maternal diet. Lastly, potential treatments that aim at shunting the progression of the pathway by inhibiting precursors to the antiapoptotic protein BCL-xL were discussed.

Keywords: pediatric brain cancer, medulloblastoma, BCL-xL, OTX2, NRL

Introduction

Medulloblastomas (MBs) are the most common and malignant pediatric brain cancers. Of the four groups, Group 3 accounts for about 27% of all medulloblastomas, has the worst prognosis, and has the greatest incidence of metastasis. This cancer arises in the vermis of the cerebellum and usually affects infants and children ages four to sixteen (Gaillard et al., 2022). Also, there is a greater predilection for males than females. Symptoms include headache, fatigue, vomiting, and disequilibrium and are similar to other childhood pathologies (DeSouza, 2014). The likeness of the disease to other childhood pathologies impacts the ability to accurately diagnose the patient and begin treatment. Currently, surgical resection, radiation, and chemotherapy are the first lines of treatment. However, at this time, some patients continue to be given only a 20% 5-year survival rate (Mahapatra and Amsbaugh, 2023).

Recent studies have begun to breakdown some of the many pathways involved in this cancer. This project attempts to model and simulate the anti-apoptotic pathway that allows the tumor to continue developing in the patients' cerebellum and may play a role in tumor metastasis. The hypothesized pathway begins with the homeobox transcription factor OTX2. Other notable proteins involved in this process include NRL, CRX, and BCL-xL. Upregulation of BCL-xL and thus the inhibition of apoptosis, in Group 3 medulloblastoma, as a result of increased concentrations of its molecular modulators was modeled and graphically supported in this project. Also, the role of maternal diet in disease incidence was investigated and it was found that there is a possible correlation between the two. Lastly, novel treatment options were suggested based on the model pathway and the information discussed.

Molecular Actors and Their Roles

BCL-xL

B-cell lymphoma-extra large (BCL-xl) is an anti-apoptotic protein that is a part of the BCL-2 family of proteins (Levesley et al., 2018). This protein family is known for regulating mitochondrial poration and dictating whether or not Cytochrome C can be released from the mitochondrion, initiating mediated cell death, or apoptosis. Interestingly, the proteins of the BCL-2 family all include a BCL-2 homology (BH) binding domain that allows these proteins to regulate each other (Levesley et al., 2018). This is important because there are both pro and anti-apoptotic proteins in the BCL-2 family.

BCL-xL plays a role in Group 3 medulloblastoma by preventing the initiation of apoptosis. It does this by binding to BAX, another BCL-2 family protein, with its BH domain (Thibaud et al., 2011). Currently, there are two hypotheses for how this process occurs. First, the binding of BCL-xL to cytosolic BAX prevents BAX from implementing itself into the outer mitochondrial membrane (OMM). The second hypothesis begins with BAX embedment into the OMM and then capping of BAX by BCL-xL, known as the “embedded together” model (Borrás et al., 2020). Both scenarios impact BAX’s ability to dimerize and create a homodimer channel in the OMM that allows for the release of Cytochrome C (Renault and Manon, 2011). Of note, Cytochrome C is the molecule that, once released and bound to Apaf-1, creating an apoptosome, activates the caspases to begin the process of apoptosis. Prevention of the release of Cytochrome C from the mitochondrion inhibits caspase activation, thus, stalling apoptosis.

The inhibition of BAX pore formation by BCL-xL can be prevented by BH domain competition. Specifically, other BCL-2 proteins such as BAD and BAK can compete with BAX at the BH domain of BCL-xL (Renault and Manon, 2011). This form of competitive inhibition

would increase the likelihood of apoptosis by allowing for the opportunity of the BAX pore to form.

Another factor that can improve the likelihood of apoptosis is changing the probability of BCL-xL expression through alternative splicing. BCL-xL RNA is the product of the gene BCL-x. This gene can be transcribed into either the BCL-xL or BCL-xS RNA. Interestingly, BCL-xS is a pro-apoptotic protein that promotes cell death by binding to BCL-xL at its BH domain and prohibiting its connection with BAX. The determining factor for the resulting RNA that is transcribed from the BCL-x gene is splicing location. The exact location of the alternative splicing options is within exon 2 of the gene (Stevens and Oltean, 2019). If the distal, compared to the proximal, 5' site of exon 2 is selected, then the BCL-xL RNA results. It has been recently shown that the inflammatory cytokine Interleukin-6 (IL-6) targets factors that regulate the alternative splicing of the BCL-2 gene (Stevens and Oltean, 2019). However, the exact mechanism of action continues to be investigated.

NRL & CRX

NRL

Neural Retina Leucine Zipper (NRL) is an important protein in the photoreceptor differentiation program. It is a basic-region leucine zipper transcription factor, is normally expressed in the retina, and is known to activate a rod-specific phototransduction cascade (Montana et al., 2011). However, in Group 3 medulloblastoma, there has been a noted overexpression of this protein (Santagata et al., 2009). Additionally, an inverse relationship between methylation, a mechanism for gene repression, and NRL expression, has been reported in this disease (Eychene and Pouponnot, 2018). Of note, it has been found that the photoreceptor

and Group 3 medulloblastoma genes are both regulated by NRL (Eychene and Pouponnot, 2018).

CRX

Cone-rod Homeobox Protein (CRX) is another protein that is critical for photoreceptor gene expression and differentiation. CRX is also a regulator of NRL and is necessary for its transcription maintenance (Montana et al., 2011). CRX, along with other proteins, like OTX2, bind to the NRL promoter region and work to initiate the transcription process. However, like NRL, it plays a role in Group 3 medulloblastoma, especially in metastatic cases (Eychene and Pouponnot, 2018).

NRL & CRX

Together, these photoreceptor proteins target BCL-xL in Group 3 medulloblastoma. NRL and CRX bind to a proximal super enhancer region that is associated with the Group 3 genes (Garancher et al., 2018). Specifically, NRL occupies the CCND2 promoter region while CRX sits closely before. The exact target nucleotide binding sites are TAATCC and TGTGA for CRX and NRL, respectively (Eychene and Pouponnot, 2018). There is also a musculo-aponeurotic-fibrosarcoma family (MAF) responsive element in the BCL-xL promoter region. MAFs are oncogenic transcription factors that regulate cell proliferation, differentiation, and apoptosis, and NRL is a part of this family of proteins (Garancher et al., 2018). Photoreceptor differentiation has been reported in this medulloblastoma and correlates with an increased RNA expression of CRX and NRL (Santagata et al., 2009). All things considered, the interactions between these proteins promote the progression of Group 3 medulloblastoma by promoting the anti-apoptotic effect of BCL-xL.

IL-6 and JAK/STAT Signaling Pathway

As mentioned before, IL-6 has been known to play a role in the alternative splicing that increases the expression of the anti-apoptotic BCL-xL over the pro-apoptotic BCL-xS. IL-6 encodes for a cytokine that is involved in inflammatory processes, and in excess, has been known to play a role in disease pathology (GeneCards, 2024). It has been reported that stem cells of the medulloblastoma tumor express IL-6 more than other cells (Westhoff et al., 2022). It is important to note that IL-6 is also an upstream regulator and activator of STAT3, a protein that helps tumor cells proliferate and survive (Sreenivasa et al., 2020). This pathway involves IL-6 binding to the receptor IL-6Ra which then dimerizes into a receptor complex that includes gp130. Through proximity mediated transactivation of gp130 and the associated JAKs, STAT3 is phosphorylated and dimerizes. STAT3 then approaches the nucleus to bind to DNA and encourages target gene expression (Sreenivasan et al., 2020). It has also been noted that STAT3 phosphorylation is not only present, but persistent in Group 3 medulloblastoma (Xiao et al., 2015). This cascade is pertinent to the tumor pathway because BCL-xL is a target of STAT3 which, alongside IL-6, further promotes upregulation of the anti-apoptotic protein and progression of the disease.

OTX2

Orthodenticle homeobox 2 (OTX2) is an important protein in normal embryonic development. The protein is a member of the Bicoid subfamily of homeodomain-containing transcription factors and plays a role in brain, craniofacial, and sensory organ development (GeneCards, 2024). In the cerebellum, granule progenitor cells have high OTX2 expression, which ends after cells begin to differentiate (Bunt et al., 2011). It is also prominent in retinal development (Garancher et al., 2018).

In Group 3 medulloblastoma, OTX2 expression is highly amplified (Cavalli et al., 2017). This is important because OTX2 plays a role in the transcriptional regulation of NRL, CRX, and IL-6. As mentioned above, OTX2 works with CRX to bind to the promoter region of NRL in order to regulate its expression (Montana et al., 2017). The specific target nucleotide sequence for OTX2 is AGGGGATTAG and the location is about 850 nucleotides before the NRL transcription region (Eychene and Pouponnot, 2018). Other targets of OTX2 are CRX and IL-6, however the exact mechanisms are not as well documented in Group 3 medulloblastoma research. Interestingly, almost a majority of OTX2 expressing tumors have been marked by the expression of photoreceptor genes (Bunt et al., 2012). Previous findings also indicate that OTX2 amplification occurs prior to metastasis, and the heightened levels are maintained throughout disease progression (Di et al., 2005). The increase in OTX2 levels furthers disease progression by upregulating the expression of the precursors to the anti-apoptotic BCL-xL protein.

Hypothesized Pathway of Molecular Events

Although the individual mechanisms between the molecular actors of Group 3 medulloblastoma have been researched, literature mapping the complete connection between the aforementioned proteins is not readily available. Therefore, this project aims to create a thorough model that displays the complex interconnections between the molecular actors in the pathway that allows this disease to develop and progress.

The hypothesized pathway model begins with OTX2, as seen in Figure 1. Alongside CRX, OTX2 aids in initiating the transcription of NRL¹. Similarly, OTX2 plays a role in the transcription of IL-6². NRL and CRX both increase the levels of BCL-xL by modulating

1. Reaction 44

2. Reaction 46

the protein's transcription³. IL-6, through the JAK/STAT pathway⁴, assures that BCL-xL, rather than BCL-xS, is transcribed from BCL-x by means of alternative splicing⁵. Without the presence of other BCL pro-apoptotic actors, such as BAD⁶, BCL-xL is able to bind to BAX. The binding of BCL-xL to BAX prevents BAX embedment into the mitochondrial outer membrane and its dimerization into the BAX pore complex⁸. Thus, cytochrome C release⁹ from the mitochondria is prohibited, inhibiting the initiation of apoptosis. The described pathway allows for the initiation and progression of BCL-xL by promoting cancer cell development and maintenance.

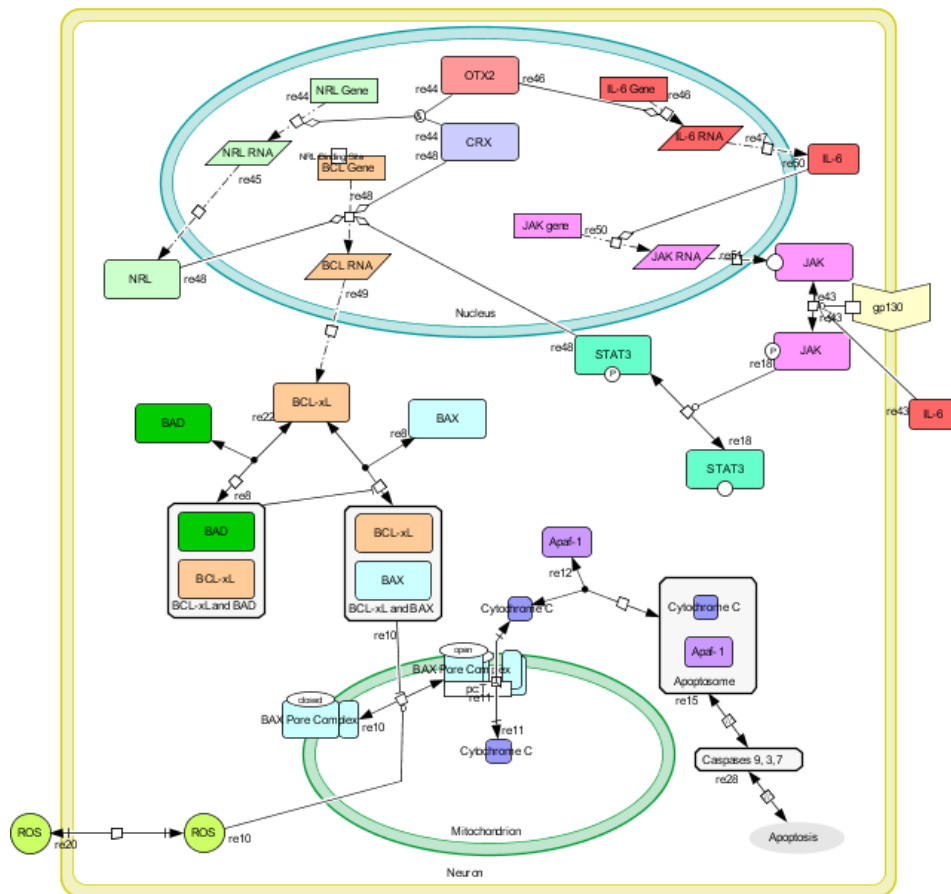


Figure 1. Project Model

- | | |
|----------------|----------------|
| 3. Reaction 48 | 7. Reaction 8 |
| 4. Reaction 43 | 8. Reaction 10 |
| 5. Reaction 48 | 9. Reaction 11 |
| 6. Reaction 22 | |

Methods

Cell Designer & SBML Squeezer

The model, Figure 1, of the hypothesized pathway discussed above was visualized using CellDesigner 4.4.2. This software models biochemical systems with respect to kinetics. CellDesigner 4.4.2 uses symbols to represent biochemical processes, such as catalysis, transcription, translation, and inhibition, and allows for interpreters to easily understand the connections between molecular factors.

Through a partnered system, SBML squeezer, known mathematical kinetic equations are applied to the visual model depending on the associations described between factors. The equations for post-translational modifications and other non-enzymatic reactions are representative of flux reactions of the proteins involved. For enzyme-catalyzed reactions, Michaelis Menten equations reflect both enzyme affinity and substrate saturation. The model's kinetic equations can be found in Appendix A.

Data

Data regarding the fold change, in log scale, of species concentrations between control and disease models of the molecular actors depicted in Figure 1 were found through investigation of prior research literature of Group 3 medulloblastoma. Research studies were found through use of R2: Genomics and Analysis and Visualization Platform created by Dr. Rogier Versteeg and others from the Academic Medical Center (AMC) in Amsterdam, Netherlands (R2: Genomics Analysis and Visualization Platform). Most studies performed analysis on tissue specimens in order to determine gene expression profiles for the target proteins. Efforts were made to find all values within the same reported data sets. A table of values used, and their sources can be found in Appendix B.

COPASI

COPASI is a complex biological pathway simulator. Use of this system allows for a visual model with kinetic equations to be run using concentration data. Through manipulation of variables and parameters, the user may simulate how the biological system runs and the pathway outcomes based on input molecular concentrations.

Results

Results were obtained by simulating the model using the “Time Course” task in COPASI. The simulation was run for 100 seconds and was graphically represented in a concentration or flux vs. time diagram. It is assumed that the time course data accurately reflects the qualitative aspects of the hypothetical model which is based on previous literature of Group 3 medulloblastoma, the applied kinetic equations, and the concentration data. The simulation was then manipulated in order to graphically visualize the effects of possible treatments that target OTX2.

Upregulation of BCL-xL concentration is evident in the project model simulation as a result of increased expression of the protein’s precursors OTX2, NRL, CRX, and IL-6. The fold-change concentration levels for the aforementioned proteins in disease tissues compared to control samples are $1.0E+12M$, $1.0E+05M$, $1.0E+10M$, and $1.0E+13M$, respectively. Figures 2 and 3 show the graphical representation of the effects of protein interactions, specifically looking at NRL concentration and BCL-xL transcription reaction flux over time in the disease model.

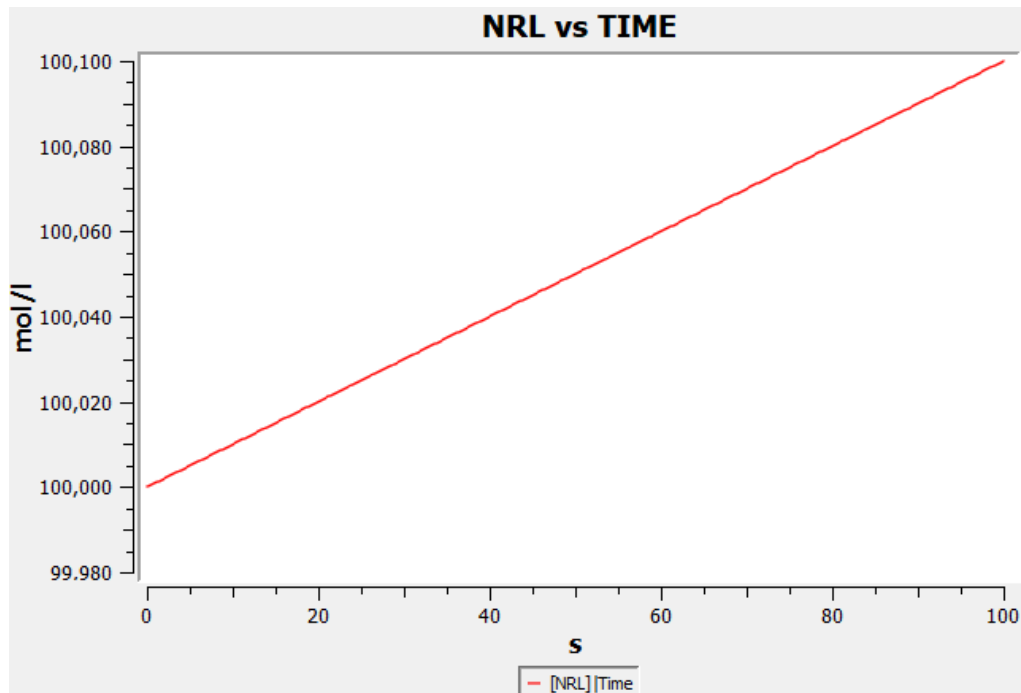


Figure 2. NRL vs TIME

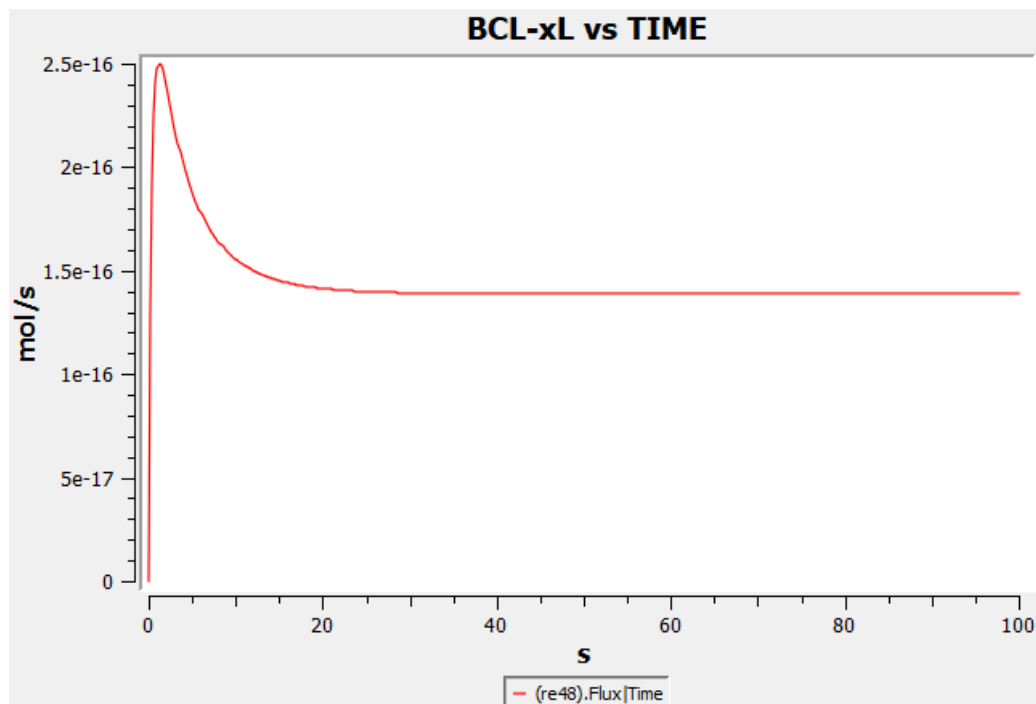


Figure 3. BCL-xL vs TIME

Figure 2 begins with an initial concentration fold change of $1.0E+10M$ for NRL. As a result of the interactions between OTX2 and CRX and their role in the transcription of NRL, the concentration of the photoreceptor protein grows linearly. Similarly, the flux reaction of BCL gene to the BCL-xL RNA¹⁰ in this model simulation grows instantaneously and then returns to an elevated state within the first 20 seconds, as seen in Figure 3. The two figures side by side show how the increase in NRL expression positively correlates with a heightened flux for the reaction representing the transcription of the BCL-xL RNA. A previous study on Group 3 medulloblastoma done by Korshunov et al. reports the r-value between NRL and BCL-xL as 0.82 with a p-value of $1.10E-03$, supporting the positive correlation between the protein expression levels seen in Figure 2 and Figure 3 (2022). The r-value is a correlation coefficient that reflects positive linear correlation, with an r-value of 1 representing perfect positive linear correlation and an r-value of 0 representing no positive linear correlation.

It has been previously reported that silencing of the OTX2 gene in Group 3 medulloblastoma prevents proliferation of cells by stopping cell cycle progression at the G0-G1 phase. Gene silencing is a technique of genetic modification that allows for the regulation of target gene expression. As a result of OTX2 silencing, many cell cycle genes are downregulated, and neuronal differentiation is increased (Bunt et al., 2012). A graphical representation of the effects of OTX2 silencing for this pathway was created using the project model and simulation.

10. Reaction 48

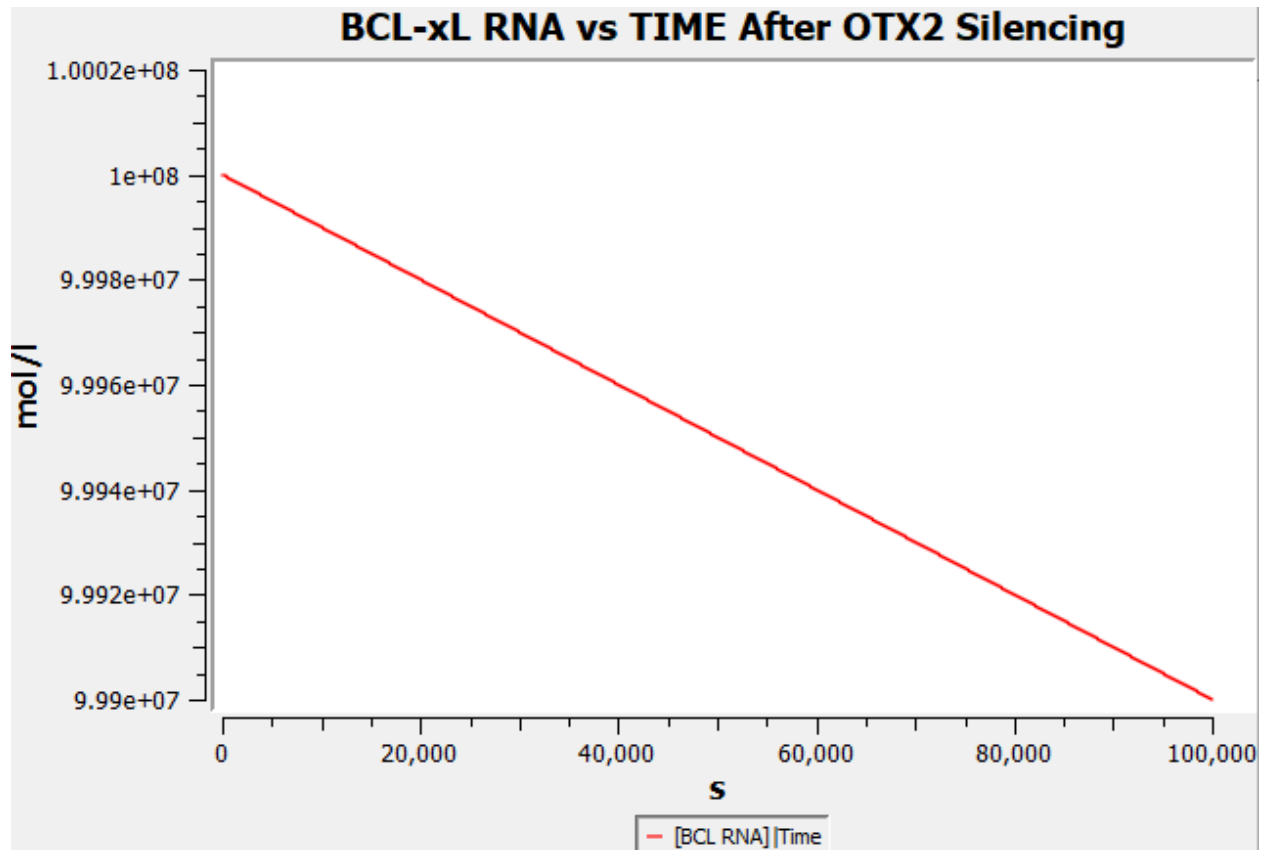


Figure 4. BCL-xL RNA vs TIME After OTX2 Silencing

Initially at $1.0E+12M$ in diseased cells, OTX2 concentration was set to $0M$, reflecting the silencing of the transcription factor. In the model simulation, repression of OTX2 caused BCL-xL expression levels to decrease, as seen in Figure 4. Although the r-value between OTX2 and BCL-xL reported by Korshunov et al., is 0.363 with a p-value of $7.62E-06$, the compounding effect on BCL-xL of OTX2 silencing in the model simulation is notable after 100,000 seconds (2022).

Limitations

Limitations to this project include the inability to extract fold change concentration data for all molecular actors from the same dataset. This may have adversely influenced the model

simulation and resulting graphs. However, efforts were made to exclude extreme data points by selecting modest concentration levels.

Discussion

Previous research into Group 3 medulloblastoma sheds light on the role of OTX2, NRL, CRX, and IL-6 in the development and progression of the cancer through promotion of the anti-apoptotic BCL-xL. This project compounds the findings of recent literature and aims to create a visual model of the disease pathway involving the aforementioned proteins. Through the use of CellDesigner 4.4.2 and its partner program SBML Squeezer, a model of the hypothesized pathway was created and mathematically described by biological kinetic equations. Using data collected from prior studies on Group 3 medulloblastoma, a simulation of the model was created using COPASI. The simulation created graphs that reflect the concentration levels of NRL and the flux of the reaction of BCL-xL transcription over time when the proteins' precursors are at heightened levels, such as in diseased cells. When OTX2 is silenced, the result is decreased BCL-xL RNA expression over time. Thus, OTX2 is a potential target for treatment in Group 3 medulloblastoma.

Maternal Diet and Disease

Unfortunately, identifying the precursors to OTX2 overexpression has been difficult. A goal of this project was to find any associations between maternal diet during pregnancy and Group 3 medulloblastoma occurrence as there is no current, singular cause associated with the disease. A study done by Bunin et al. in 2005 polled biological female parents of children with Group 3 medulloblastoma. The investigators looked at eight different food groups which included the following: dairy, fruit without juices, fruit with juices, citrus fruit and juices, vegetables without juices or soup, vegetables with juices or soup, cured meat and fish, and fresh

meat. The researchers also asked about individual foods such as citrus fruits, French fries, corn, beans, nonchocolate candy, diet soda, and chili peppers.

After collecting data on types of foods eaten and the frequency of intake, the investigators analyzed the odds ratio (ORs) of food to disease incidence, with a lower OR being indicative of lower disease occurrence. It was found that the foods with the lowest ORs were canned, dried, or frozen apricots, peaches, and nectarines. This is important to North American cultures as canned peaches accounted for around 80% of the not-fresh category of food consumed at the time of the study (Bunin et al., 2005). Other foods with low ORs included non-citrus fruit juices, corn and lima beans/peas, and winter squash. The food group with the lowest ORs was fruit juices and there was a notable inverse association between the two factors. For nutrients, there was a slight decrease in ORs for Vitamin C and when using animal protein.

However, there were many foods and food groups with increased ORs for Group 3 medulloblastoma. For example, French fries, nonchocolate candy, and diet soda all had increased ORs. Chili peppers also had increased ORs which positively correlated with increased consumption. For fried foods in general, there was a slight increase in ORs when eating these foods at home at least once a week. The nutrient with an increased OR was vegetable fat. Lastly, cured meats had no association to Group 3 medulloblastoma incidence.

The researchers discussed a few possible mechanisms for increased disease occurrence after maternal ingestion of French fries and diet soda. For French fries, the authors noted that acrylamide, a nerve toxin and animal carcinogen, is released when carbohydrate foods are cooked at high temperatures. For diet soda, at the time of the polling, aspartame, an artificial sweetener, was common in these beverages. The researchers also note that there is a correlation between the introduction of aspartame into the United States food supply 1981 and the increased

occurrence of brain tumors afterwards. However, for both cases, the investigators note the scenarios are unlikely to contribute to Group 3 medulloblastoma and the exact biochemical mechanisms of action for foods in maternal diet and the cancer are unknown.

Another study conducted by Wulff et al., in 2020 investigated the role of O-GlcNAc in maternal diet and OTX2. O-GlcNAc is a glucose rheostat that plays a role in cell signaling (Wulff et al., 2020). UDP-GlcNAc is a primary substrate for the rheostat and its expression levels reflect the levels of extracellular glucose. OTX2 is a major O-GlcNAcylated protein, and O-GlcNAc regulates the activity and localization of the homeobox transcription factor during brain development. More specifically, the repression domain of OTX2 is highly O-GlcNAcylated, affecting the transcription of OTX2 and its phosphorylation sites. It has been reported that OTX2 is dysregulated in hyper-O-GlcNAcylated models (Wulff et al., 2020). Thus, the investigators believe that OTX2 dysregulation by O-GlcNAcylation during development of the cerebellum leads way for Group 3 medulloblastoma incidence.

Lastly, although not yet reflected in human models, a previous study conducted by Micheloni et al. in 2021 looked at how a soy diet induces intestinal inflammation in adult Zebrafish and how OTX plays a role in this process. The investigators used Zebrafish because they have a simpler gut structure and have been a trusted animal model for other human diseases such as enterocolitis and irritable bowel diseases. The diet in question was of soya bean meal (SBM), which is a common meal for aquatic species in agriculture. The authors note that the OTXs play an important role in the gut in gastrointestinal diseases. OTX2, specifically, is mostly upregulated in the neurons of previous gut disease models and is in association with neuronal nitric oxide synthase (Micheloni et al., 2021).

It was found that saponin, a steroid glycoside, is contained in SBM and triggers an inflammatory response in the distal intestine. There was also a significant change in NOS1 mRNA expression which shows that saponin significantly increased oxidative stress on the intestinal wall and its resident neurons (Micheloni et al., 2021). Chronic inflammation was noted after four weeks of SBM. Also, the OTX genes were upregulated in the first two weeks after SBM was given to model zebrafish. Thus, the investigators believe that the OTX genes are early markers of intestinal injury and inflammation.

Treatments

Medicine

Previous research has identified potential medicinal treatments that aim to inhibit OTX2. One such treatment is all-trans retinoic acid. In a study conducted by Di et al., the concentration of OTX2 in a Group 3 medulloblastoma cell culture was reported to be amplified more than ten-fold (2005). All-trans retinoic acid is an exogenous retinoid that is one of the nuclear acting lipid soluble hormones that can displace or repress OTX2. The retinoid impacts OTX2 expression by cis-acting elements on the OTX2 promoter (Di et al., 2005). In the study, when all-trans retinoic acid was applied to diseased cells, medulloblastoma cell proliferation was inhibited. However, the exact mechanism of action is not known. Evidence from the Di et al. study with all-trans retinoic acid along with the results of the project model simulation after silencing of OTX2 suggest that further efforts should be made to experiment with inhibitors of OTX2 in order to treat Group 3 medulloblastoma.

Another medicinal treatment option that may help combat the growth and proliferation of Group 3 medulloblastoma tumors is the use of a BH3 mimetic. As mentioned before, all BCL-2 family proteins contain a BH binding domain where the proteins can interact to regulate the

activity of each other. Applying BAD, the BCL-2 agonist of cell death, creates competition with BAX for BCL-xL's BH binding domain (Levesley et al., 2018). Thus, inhibiting BCL-xL's ability to bind to BAX allows for apoptosis to occur, shunting tumor cell survival. This target mechanism for treatment is supported by the pathway outlined in the project model.

Diet

The findings of the aforementioned studies provide insight into foods that may be increasing the risk of Group 3 medulloblastoma occurrence. Thus, efforts should be made to further investigate mainstream foods and their impact on maternal and fetal health, in the same way that medications and recreational substances have been. As supported above, intake of foods or juices with high fruit content should be suggested while frequent ingestion of fried foods, foods that increase extracellular glucose, and foods containing saponin should be discouraged. A list of diet recommendations that is widely available may be pertinent to keeping parents and their children safe and healthy not only from Group 3 medulloblastoma, but other cancers and diseases as well.

Additionally, investigation into ethnic and cultural foods and practices should be considered. In the Bunin et al. study, it was reported that chili peppers had high ORs with disease incidence (2005). The investigators noted that the poll included both non-Spanish and Spanish speakers in North America. When the Spanish speaking population was removed, the presence of chili pepper influence was still notable. However, it was reported that increased intake of chili peppers correlated with a greater OR. The researchers agree that efforts should be made to further investigate the role of ethnic and cultural foods and practices in Group 3 medulloblastoma incidence.

Lastly, it may be important to consider social/economic class and environment in future studies that seek to identify foods in maternal diet that are correlated with Group 3 medulloblastoma incidence. The Bunin et al. study mentioned that social class may have biased the results of the study as consumption of the foods with the lowest ORs was greater than in their previous studies. It was noted that many of the families polled made at least \$50,000 year (Bunin et al., 2005). Thus, they suggest that access to these foods may vary between different social classes. Also, some families are located within food deserts, or areas where access to healthy food options is limited (Caporuscio, 2024). Factors like these should also be further investigated to see if there is a higher or lower prevalence of Group 3 medulloblastoma in these populations.

Conclusion

In conclusion, this project sought to model one of the many pathways in Group 3 medulloblastoma, provide graphical support for the model interactions through pathway simulation, identify a connection between maternal diet and disease, and discuss possible treatments. The project model shows the interconnected pathway between OTX2, NRL, CRX, IL-6, other associated proteins, and BCL-xL. It was shown and supported that upregulation of the precursors to the anti-apoptotic protein BCL-xL, such as NRL, allows for the development and progression of Group 3 medulloblastoma. OTX2 silencing as a potential treatment option for this disease was also supported graphically through the model pathway simulation.

A connection was found between maternal diet and the incidence of Group 3 medulloblastoma. As in other neurodegenerative diseases, the gut and its microbiome influence the health of our brains. Therefore, it is important to educate the population about what foods improve cognitive function and which increase the risks of neurodegenerative diseases, such as Group 3 medulloblastoma. Also, treatments that target OTX2 and other precursors of BCL-xL

may have a greater efficacy than the current treatment options which include radiation, chemotherapy, and surgical resection. Future efforts should be made to further investigate treatment options that target the project hypothesized pathway and to identify other external factors that may increase the risk of developing Group 3 medulloblastoma.

References

- Borrás, C., Mas-Bargues, C., Román-Domínguez, A., Sanz-Ros, J., Gimeno-Mallench, L., Inglés, M., Gambini, J., & Viña, J. (2020). BCL-xL, a mitochondrial protein involved in successful aging: From *C. elegans* to human centenarians. *International Journal of Molecular Sciences*, *21*(2), 418-. <https://doi.org/10.3390/ijms21020418>
- Bunin GR, Kushi LH, Gallagher PR, Rorke-Adams LB, McBride ML, Cnaan A. (2005) Maternal diet during pregnancy and its association with medulloblastoma in children: a children's oncology group study (United States). *Cancer Causes Control*, *16*(7):877-91. doi: 10.1007/s10552-005-3144-7. PMID: 16132798.
- Bunt J, Hasselt NE, Zwijnenburg DA, Hamdi M, Koster J, Versteeg R, Kool M. (2012) OTX2 directly activates cell cycle genes and inhibits differentiation in medulloblastoma cells. *Int J Cancer*, *131*(2):E21-32. doi: 10.1002/ijc.26474. Epub 2011 Nov 8. PMID: 21964830.
- Caporuscio, J. (n.d.). Food deserts: Definition, effects, and solutions. Retrieved from <https://www.medicalnewstoday.com/articles/what-are-food-deserts>
- DeSouza, R. M., Jones, B. R., Lowis, S. P., & Kurian, K. M. (2014). Pediatric medulloblastoma - update on molecular classification driving targeted therapies. *Frontiers in oncology*, *4*, 176. <https://doi.org/10.3389/fonc.2014.00176>
- Di C, Liao S, Adamson DC, Parrett TJ, Broderick DK, Shi Q, Lengauer C, Cummins JM, Velculescu VE, Fults DW, McLendon RE, Bigner DD, Yan H. (2005) Identification of OTX2 as a medulloblastoma oncogene whose product can be targeted by all-trans retinoic acid. *Cancer Res.*, *65*(3):919-24. PMID: 15705891.

Eychène, A. and Pouponnot, C. (2018). *The photoreceptor program in group 3 medulloblastoma: Role of the TFs NRL and CRX*

Gaillard F, Jones J, Sharma R, et al. Medulloblastoma, group 3. Reference article,

Radiopaedia.org (Accessed on 29 Mar 2024) <https://doi.org/10.53347/rID-41025>

Garancher A, Lin C, Morabito M, Larcher M, Rocques N, Miquel C, Habeler C, Puget S, Ayrault O, Wechsler-Reya R, Bourdeaut F, Eychene A, Northcott P, Pouponnot C. (2017) MEDU-24. INSTRUMENTAL ROLE OF THE PHOTORECEPTOR PROGRAM IN GROUP 3 MEDULLOBLASTOMA THROUGH THE TRANSCRIPTION FACTOR NRL. *Neuro Oncol.*, 19(Suppl 4):iv42. doi: 10.1093/neuonc/nox083.174. Epub 2017 May 31. PMID: PMC5475149.

Stelzer G, Rosen R, Plaschkes I, Zimmerman S, Twik M, Fishilevich S, Iny Stein T, Nudel R, Lieder I, Mazor Y, Kaplan S, Dahary, D, Warshawsky D, Guan - Golan Y, Kohn A, Rappaport N, Safran M, and Lancet D. *The GeneCards Suite: From Gene Data Mining to Disease Genome Sequence Analyses* (PMID: 27322403; Citations: 3,096) *Current Protocols in Bioinformatics*(2016), 54:1.30.1 - 1.30.33.doi: 10.1002 / cpbi.5 [PDF]

Levesley J, Steele L, Brüning-Richardson A, Davison A, Zhou J, Ding C, Lawler S, Short SC. (2018) Selective BCL-XL inhibition promotes apoptosis in combination with MLN8237 in medulloblastoma and pediatric glioblastoma cells. *Neuro Oncol.*, 20(2):203-214. doi: 10.1093/neuonc/nox134. PMID: 29016820; PMID: PMC7059858.

Mahapatra S, Amsbaugh MJ. Medulloblastoma. [Updated 2023 Jun 26]. In: StatPearls [Internet]. Treasure Island (FL): StatPearls Publishing; 2024 Jan-. Available from: <https://www.ncbi.nlm.nih.gov/books/NBK431069/>

- Micheloni, G., Carnovali, M., Millefanti, G., Rizzetto, M., Moretti, V., Montalbano, G., Acquati, F., Giaroni, C., Valli, R., Costantino, L., Ferrara, F., Banfi, G., Mariotti, M., & Porta, G. (2022). Soy diet induces intestinal inflammation in adult Zebrafish: Role of OTX and P53 family. *International Journal of Experimental Pathology*, *103*(1), 13–22.
<https://doi.org/10.1111/iep.12420>
- Montana CL, Lawrence KA, Williams NL, Tran NM, Peng GH, Chen S, Corbo JC. (2011) Transcriptional regulation of neural retina leucine zipper (Nrl), a photoreceptor cell fate determinant. *J Biol Chem.*, *286*(42):36921-31. doi: 10.1074/jbc.M111.279026. Epub 2011 Aug 24. PMID: 21865162; PMCID: PMC3196091.
- Renault TT, Manon S. (2011) Bax: Addressed to kill. *Biochimie.*, *93*(9):1379-91. doi: 10.1016/j.biochi.2011.05.013. Epub 2011 May 30. PMID: 21641962.
- Santagata S, Maire CL, Idbah A, Geffers L, Correll M, et al. (2009) CRX Is a Diagnostic Marker of Retinal and Pineal Lineage Tumors. *PLoS ONE*, *4*(11): e7932.
doi:10.1371/journal.pone.0007932
- Sreenivasan L, Wang H, Yap SQ, Leclair P, Tam A, Lim CJ. (2020) Autocrine IL-6/STAT3 signaling aids development of acquired drug resistance in Group 3 medulloblastoma. *Cell Death Dis.*, *11*(12):1035. doi: 10.1038/s41419-020-03241-y. PMID: 33279931; PMCID: PMC7719195.
- Stevens M, Oltean S. (2019) Modulation of the Apoptosis Gene Bcl-x Function Through Alternative Splicing. *Front Genet.*, *10*:804. doi: 10.3389/fgene.2019.00804. PMID: 31552099; PMCID: PMC6743414.

- Westhoff, M.-A.; Schuler-Ortoli, M.; Zerrinius, D.; Hadzalic, A.; Schuster, A.; Strobel, H.; Scheuerle, A.; Wong, T.; Wirtz, C.R.; Debatin, K.-M.; et al. (2022) Bcl-XL but Not Bcl-2 Is a Potential Target in Medulloblastoma Therapy. *Pharmaceuticals*, 15, 91. <https://doi.org/10.3390/ph15010091>
- Wulff, E. A., Boakye, J., Berendt, R., Hanover, J. A., & Stichelen, S. O. (2020). Linking Maternal Sugar Consumption to Progenies' Developmental Defects: A Focus on OTX2's O-GlcNAcylation. *The FASEB Journal*, 34(S1), 1–1. <https://doi.org/10.1096/fasebj.2020.34.s1.03604>
- Xiao, H. (2015). A novel small molecular STAT3 inhibitor, LY5, inhibits cell viability, cell migration, and angiogenesis in medulloblastoma cells. *Journal of Biological Chemistry*, 290(6), 3418–3429.
- Zhang, M., Zheng, J., Nussinov, R. et al. (2017). Release of Cytochrome C from Bax Pores at the Mitochondrial Membrane. *Sci Rep* 7, 2635. <https://doi.org/10.1038/s41598-017-02825-7>

Appendix A

$$\begin{aligned}
 \frac{d([\text{"NRL Gene"}] \cdot V_{\text{Nucleus}})}{dt} &= -V_{\text{Nucleus}} \cdot \left(\frac{\frac{[\text{OTX2}]}{kA_{11_s1} + [\text{OTX2}] \cdot [\text{CRX}]} \cdot kI_{11_s1}}{kA_{11_s2} + [\text{CRX}] \cdot kI_{11_s2}} \cdot kass_{11}}{V_{\text{Nucleus}}} \right) \\
 \frac{d([\text{"NRL RNA"}] \cdot V_{\text{Nucleus}})}{dt} &= +V_{\text{Nucleus}} \cdot \left(\frac{\frac{[\text{OTX2}]}{kA_{11_s1} + [\text{OTX2}] \cdot [\text{CRX}]} \cdot kI_{11_s1}}{kA_{11_s2} + [\text{CRX}] \cdot kI_{11_s2}} \cdot kass_{11}}{V_{\text{Nucleus}}} \right) \\
 &\quad - (kass_{12}) \\
 \frac{d([\text{NRL}] \cdot V_{\text{Neuron}})}{dt} &= + (kass_{12}) \\
 \frac{d([\text{"BCL Gene"}] \cdot V_{\text{Nucleus}})}{dt} &= - \left(\frac{\frac{[\text{NRL}]}{kA_{15_s5} + [\text{NRL}] \cdot [\text{STAT3_2}]} \cdot [\text{CRX}]}{kA_{15_s47} + [\text{STAT3_2}] \cdot kI_{15_s5}} \cdot kI_{15_s47}}{kI_{15_s5} + [\text{NRL}] \cdot kI_{15_s2}} \cdot kass_{15}}{kI_{15_s2} + [\text{CRX}]} \right) \\
 \frac{d([\text{"BCL RNA"}] \cdot V_{\text{Nucleus}})}{dt} &= + \left(\frac{\frac{[\text{NRL}]}{kA_{15_s5} + [\text{NRL}] \cdot [\text{STAT3_2}]} \cdot [\text{CRX}]}{kA_{15_s47} + [\text{STAT3_2}] \cdot kI_{15_s5}} \cdot kI_{15_s47}}{kI_{15_s5} + [\text{NRL}] \cdot kI_{15_s2}} \cdot kass_{15}}{kI_{15_s2} + [\text{CRX}]} \right) \\
 &\quad - (kass_{16})
 \end{aligned}$$

$$\begin{aligned}
\frac{d([\text{"BCL-xL"}] \cdot V_{\text{Neuron}})}{d t} &= -V_{\text{Neuron}} \cdot \left(\frac{\text{kass}_1 \cdot [\text{"BAX"}] \cdot [\text{"BCL-xL"}] - \text{kdiss}_1}{V_{\text{Neuron}}} \right) \\
&\quad - V_{\text{Neuron}} \cdot \left(\frac{\text{kass}_8 \cdot [\text{"BAD"}] \cdot [\text{"BCL-xL"}]}{V_{\text{Neuron}}} \right) \\
&\quad + V_{\text{Neuron}} \cdot \left(\frac{\text{kdiss}_8 \cdot [\text{"BCL-xL and BAD"}]}{V_{\text{Neuron}}} \right) \\
&\quad + (\text{kass}_{16}) \\
\frac{d([\text{"JAK gene"}] \cdot V_{\text{Nucleus}})}{d t} &= \left(\frac{[\text{"IL-6\{Neuron\}"}] \cdot \text{kI}_{17_s12}}{\text{kA}_{17_s12} + [\text{"IL-6\{Neuron\}"}]} \cdot \text{kass}_{17} \right) \\
\frac{d([\text{"JAK RNA"}] \cdot V_{\text{Nucleus}})}{d t} &= + \left(\frac{[\text{"IL-6\{Neuron\}"}] \cdot \text{kI}_{17_s12}}{\text{kI}_{17_s12} + [\text{"IL-6\{Neuron\}"}]} \cdot \text{kass}_{17} \right) \\
&\quad - (\text{kass}_{18}) \\
\frac{d([\text{STAT3}] \cdot V_{\text{Neuron}})}{d t} &= -V_{\text{Neuron}} \cdot \left(\frac{[\text{JAK}_2] \cdot \frac{\text{kcatp}_6}{\text{kM}_{6_s13}} \cdot [\text{STAT3}]}{1 + \frac{[\text{STAT3}]}{\text{kM}_{6_s13}} + \frac{[\text{STAT3}_2]}{\text{kM}_{6_s47}}} \right) \\
&\quad + V_{\text{Neuron}} \cdot \left(\frac{[\text{JAK}_2] \cdot \frac{\text{kcatn}_6}{\text{kM}_{6_s47}} \cdot [\text{STAT3}_2]}{1 + \frac{[\text{STAT3}]}{\text{kM}_{6_s13}} + \frac{[\text{STAT3}_2]}{\text{kM}_{6_s47}}} \right) \\
\frac{d([\text{"BCL-xL and BAX"}] \cdot V_{\text{Neuron}})}{d t} &= + V_{\text{Neuron}} \cdot \left(\frac{\text{kass}_1 \cdot [\text{"BAX"}] \cdot [\text{"BCL-xL"}] - \text{kdiss}_1}{V_{\text{Neuron}}} \right) \\
\frac{d([\text{"BAX"}] \cdot V_{\text{Neuron}})}{d t} &= -V_{\text{Neuron}} \cdot \left(\frac{\text{kass}_1 \cdot [\text{"BAX"}] \cdot [\text{"BCL-xL"}] - \text{kdiss}_1}{V_{\text{Neuron}}} \right) \\
\frac{d([\text{"Apaf-1"}] \cdot V_{\text{Neuron}})}{d t} &= -V_{\text{Neuron}} \cdot \left(\frac{\text{kass}_4 \cdot [\text{"Cytochrome C\{Neuron\}"}] \cdot [\text{"Apaf-1"}]}{V_{\text{Neuron}}} \right) \\
&\quad + V_{\text{Neuron}} \cdot \left(\frac{\text{kdiss}_4 \cdot [\text{Apoptosome}]}{V_{\text{Neuron}}} \right) \\
\frac{d([\text{"Cytochrome C\{Mitochondrion\}"}] \cdot V_{\text{Mitochondrion}})}{d t} &= -(\text{kass}_3 \cdot [\text{"Cytochrome C\{Mitochondrion\}"}] \cdot [\text{"BAX Pore Complex}_2"]) \\
&\quad + (\text{kdiss}_3 \cdot [\text{"Cytochrome C\{Neuron\}"}] \cdot [\text{"BAX Pore Complex}_2"]) \\
\frac{d([\text{"Cytochrome C\{Neuron\}"}] \cdot V_{\text{Neuron}})}{d t} &= +(\text{kass}_3 \cdot [\text{"Cytochrome C\{Mitochondrion\}"}] \cdot [\text{"BAX Pore Complex}_2"]) \\
&\quad - (\text{kdiss}_3 \cdot [\text{"Cytochrome C\{Neuron\}"}] \cdot [\text{"BAX Pore Complex}_2"]) \\
&\quad - V_{\text{Neuron}} \cdot \left(\frac{\text{kass}_4 \cdot [\text{"Cytochrome C\{Neuron\}"}] \cdot [\text{"Apaf-1"}]}{V_{\text{Neuron}}} \right) \\
&\quad + V_{\text{Neuron}} \cdot \left(\frac{\text{kdiss}_4 \cdot [\text{Apoptosome}]}{V_{\text{Neuron}}} \right)
\end{aligned}$$

$$\frac{d([\text{"Caspases 9, 3, 7"}] \cdot V_{\text{Neuron}})}{d t}$$

$$= +V_{\text{Neuron}} \cdot \left(\frac{\text{kass}_5 \cdot [\text{Apoptosome}]}{V_{\text{Neuron}}} \right) \\ -V_{\text{Neuron}} \cdot \left(\frac{\text{kdiss}_5 \cdot [\text{"Caspases 9, 3, 7"}]}{V_{\text{Neuron}}} \right) \\ -V_{\text{Neuron}} \cdot \left(\frac{\text{kass}_9 \cdot [\text{"Caspases 9, 3, 7"}]}{V_{\text{Neuron}}} \right) \\ +V_{\text{Neuron}} \cdot \left(\frac{\text{kdiss}_9 \cdot [\text{Apoptosis}]}{V_{\text{Neuron}}} \right)$$

$$\frac{d([\text{"BAX Pore Complex"}] \cdot V_{\text{Mitochondrion}})}{d t}$$

$$= +(\text{kdiss}_2 \cdot [\text{"BAX Pore Complex}_2"] \cdot [\text{ROS}\{\text{Neuron}\}]) \\ -(\text{kass}_2 \cdot [\text{"BAX Pore Complex"}] \cdot [\text{ROS}\{\text{Neuron}\}])$$

$$\frac{d([\text{Apoptosome}] \cdot V_{\text{Neuron}})}{d t}$$

$$= +V_{\text{Neuron}} \cdot \left(\frac{\text{kass}_4 \cdot [\text{"Cytochrome C}\{\text{Neuron}\}] \cdot [\text{"Apaf-1"}]}{V_{\text{Neuron}}} \right) \\ -V_{\text{Neuron}} \cdot \left(\frac{\text{kdiss}_4 \cdot [\text{Apoptosome}]}{V_{\text{Neuron}}} \right) \\ -V_{\text{Neuron}} \cdot \left(\frac{\text{kass}_5 \cdot [\text{Apoptosome}]}{V_{\text{Neuron}}} \right) \\ +V_{\text{Neuron}} \cdot \left(\frac{\text{kdiss}_5 \cdot [\text{"Caspases 9, 3, 7"}]}{V_{\text{Neuron}}} \right)$$

$$\frac{d([\text{STAT3}_2] \cdot V_{\text{Neuron}})}{d t}$$

$$= +V_{\text{Neuron}} \cdot \left(\frac{\frac{[\text{JAK}_2] \cdot \frac{\text{kcatp}_6}{\text{kM}_6_{\text{s13}}} \cdot [\text{STAT3}]}{1 + \frac{[\text{STAT3}]}{\text{kM}_6_{\text{s13}}} + \frac{[\text{STAT3}_2]}{\text{kM}_6_{\text{s47}}}}}{V_{\text{Neuron}}} \right) \\ -V_{\text{Neuron}} \cdot \left(\frac{\frac{[\text{JAK}_2] \cdot \frac{\text{kcatn}_6}{\text{kM}_6_{\text{s47}}} \cdot [\text{STAT3}_2]}{1 + \frac{[\text{STAT3}]}{\text{kM}_6_{\text{s13}}} + \frac{[\text{STAT3}_2]}{\text{kM}_6_{\text{s47}}}}}{V_{\text{Neuron}}} \right)$$

$$\frac{d([\text{Apoptosis}] \cdot V_{\text{Neuron}})}{d t}$$

$$= +V_{\text{Neuron}} \cdot \left(\frac{\text{kass}_9 \cdot [\text{"Caspases 9, 3, 7"}]}{V_{\text{Neuron}}} \right) \\ -V_{\text{Neuron}} \cdot \left(\frac{\text{kdiss}_9 \cdot [\text{Apoptosis}]}{V_{\text{Neuron}}} \right)$$

$$\frac{d([\text{"IL-6}\{\text{Neuron}\}"] \cdot V_{\text{Neuron}})}{d t}$$

$$= +(\text{kass}_{14})$$

$$\frac{d([\text{ROS}\{\text{default}\}] \cdot V_{\text{default}})}{d t}$$

$$= -(\text{kass}_7 \cdot [\text{ROS}\{\text{default}\}]) \\ +(\text{kdiss}_7 \cdot [\text{ROS}\{\text{Neuron}\}])$$

$$\frac{d([\text{ROS}\{\text{Neuron}\}] \cdot V_{\text{Neuron}})}{d t}$$

$$= +(\text{kass}_7 \cdot [\text{ROS}\{\text{default}\}]) \\ -(\text{kdiss}_7 \cdot [\text{ROS}\{\text{Neuron}\}])$$

$$\begin{aligned}
\frac{d([\text{BAD}] \cdot V_{\text{Neuron}})}{d t} &= -V_{\text{Neuron}} \cdot \left(\frac{\text{kass_8} \cdot [\text{BAD}] \cdot [\text{"BCL-xL"}]}{V_{\text{Neuron}}} \right) \\
&\quad + V_{\text{Neuron}} \cdot \left(\frac{\text{kdis_8} \cdot [\text{"BCL-xL and BAD"}]}{V_{\text{Neuron}}} \right) \\
\frac{d([\text{"BCL-xL and BAD"}] \cdot V_{\text{Neuron}})}{d t} &= +V_{\text{Neuron}} \cdot \left(\frac{\text{kass_8} \cdot [\text{BAD}] \cdot [\text{"BCL-xL"}]}{V_{\text{Neuron}}} \right) \\
&\quad - V_{\text{Neuron}} \cdot \left(\frac{\text{kdis_8} \cdot [\text{"BCL-xL and BAD"}]}{V_{\text{Neuron}}} \right) \\
\frac{d([\text{"IL-6 Gene"}] \cdot V_{\text{Nucleus}})}{d t} &= -V_{\text{Nucleus}} \cdot \left(\frac{\text{kass_13}}{V_{\text{Nucleus}}} \right) \\
\frac{d([\text{"IL-6 RNA"}] \cdot V_{\text{Nucleus}})}{d t} &= +V_{\text{Nucleus}} \cdot \left(\frac{\text{kass_13}}{V_{\text{Nucleus}}} \right) \\
&\quad - (\text{kass_14}) \\
\frac{d([\text{JAK}] \cdot V_{\text{Neuron}})}{d t} &= - \left(\frac{[\text{"IL-6\{default\}"}] \cdot \text{kI_10_s62}}{\text{kA_10_s62} + [\text{"IL-6\{default\}"}]} \cdot \text{kass_10} \cdot [\text{JAK}] \cdot [\text{gp130}] \right) \\
&\quad + \left(\frac{[\text{"IL-6\{default\}"}] \cdot \text{kI_10_s62}}{\text{kI_10_s62} + [\text{"IL-6\{default\}"}]} \cdot \text{kdis_10} \cdot [\text{JAK_2}] \cdot [\text{gp130}] \right) \\
&\quad + (\text{kass_18}) \\
\frac{d([\text{JAK_2}] \cdot V_{\text{Neuron}})}{d t} &= + \left(\frac{[\text{"IL-6\{default\}"}] \cdot \text{kI_10_s62}}{\text{kA_10_s62} + [\text{"IL-6\{default\}"}]} \cdot \text{kass_10} \cdot [\text{JAK}] \cdot [\text{gp130}] \right) \\
&\quad - \left(\frac{[\text{"IL-6\{default\}"}] \cdot \text{kI_10_s62}}{\text{kI_10_s62} + [\text{"IL-6\{default\}"}]} \cdot \text{kdis_10} \cdot [\text{JAK_2}] \cdot [\text{gp130}] \right) \\
\frac{d([\text{"BAX Pore Complex_2"}] \cdot V_{\text{Mitochondrion}})}{d t} &= -(\text{kdis_2} \cdot [\text{"BAX Pore Complex_2"}] \cdot [\text{ROS\{Neuron\}}]) \\
&\quad + (\text{kass_2} \cdot [\text{"BAX Pore Complex"}] \cdot [\text{ROS\{Neuron\}}])
\end{aligned}$$

Appendix B

Molecular Actors and Concentrations in Disease Models as Fold Change from Normal Models

Molecular Actor	Fold Change	p-value	Source
NRL	1.00E+05	1.16E-05	doi:10.1038/nm.3553
CRX	1.00E+10	4.76E-02	doi:10.1038/nm.3553
OTX2	1.00E+12	1.03E-14	doi:10.1038/nm.3553
IL-6	1.00E+13	1.02E-05	doi: 10.1158/2326-6066.CIR-15-0061
JAK	1.00E+03	6.54E-05	doi: 10.1158/2326-6066.CIR-15-0061
STAT3	1.00E+01	3.72E-06	doi: 10.1158/2326-6066.CIR-15-0061
BCL-xL	1.00E+08	Not disclosed	doi:10.1038/nm.3553